Phonon transport simulations in low-dimensional, disordered graphene nanoribbons

Neophytos Neophytou
School of Engineering,
University of Warwick,
Coventry, CV4 7AL, UK
N.Neophytou@warwick.ac.uk

Hossein Karamitaheri
Department of Electrical Engineering,
University of Kashan,
Kashan 87317-53153, Iran

***Abstract*— In this work we investigate phonon transport in low-dimensional, disordered armchair graphene nanoribbons (GNRs) in order to illuminate phonon transport effects in 1D disordered systems. We use the non-equilibrium Green's function (NEGF) simulation technique for transport, coupled to the force constant method for obtaining the phonon bandstructure. We focus on how different parts of the phonon spectrum are influenced by geometrical confinement and line edge roughness. In the ballistic case, phonons throughout the entire phonon energy spectrum contribute to thermal transport. With the introduction of line edge roughness, the phonon transmission is reduced, but quantitatively and qualitatively in different ways throughout the energy spectrum. We identify how each region of the spectrum reacts to low-dimensionality and disorder, and elaborate on how phonon transport is affected by that. We explain how and when phonons in different energies within the spectrum flow either ballistically, diffusively, or become localized depending on features of the channel geometry. Finally, we derive exponents related to the length and width dependence of the thermal transport in the GNRs under the influence of line-etch roughness. Our results could provide generic features of thermal transport in different classes of low-dimensional materials beyond GNRs, and could help understand heat transport at the nanoscale better.**

Keywords*— *theory; simulation; phonon transport; graphene nanoribbons; low-dimensionality; NEGF

I. Introduction

Carbon related materials such as graphene, nanotubes, and graphene nanoribbons (GNRs) have huge thermal conductivities in their pristine form, reaching values as high as of 3080-5150 W/m K at room temperature, and have attracted significant attention both for fundamental research as well as for technological applications [1-9]. Ultra-narrow graphene nanoribbons have been shown to retain at some degree the remarkable thermal properties of graphene, however, the presence of edges can determine its heat transport properties [7, 10-12]. Even a small degree of disorder can drastically degrade this superior thermal conductivity. Several works have indeed shown that the transport properties of low-dimensional systems are significantly degraded by the introduction of scattering centers and localized states [7, 9, 10, 13-15]. For example, two orders of magnitude reduction in thermal conductivity has been reported for roughened GNRs, but also for several other low-dimensional materials. For certain applications, such as heat management, this is detrimental, but for other applications such as thermoelectric materials, reduction in the thermal conductivity is beneficial as it significantly improves the thermoelectric conversion efficiency, and thus, it creates interest from technological point of view as well [9, 16, 17].

Several works attempt to compute and understand the thermal properties of low-dimensional materials using various methods, depending on the size of the systems and the computational complexity it involves. These are molecular dynamics (MD) [18-22], the Boltzmann Transport Equation (BTE) for phonons using scattering rates based on the single mode relaxation time approximation (SMRTA) [23-26], the non-equilibrium Green's function (NEGF) method [27-33], and the Landauer method [34-36], and even more simplified semi-analytical methods based on the Casimir formula to describe boundary scattering [37, 38].

Thermal transport studies in graphene and GNRs, specifically, are in general more computationally tangible, and could illuminate the physics of phonon transport at the nanoscale, which reveals features distinctly different from bulk materials. For example, several experimental and theoretical works suggest that the thermal conductivity could deviate from Fourier's law [39-41]. It was observed that it grows monotonically with channel length before it saturates at large channel lengths, even lengths significantly larger than the average mean-free-path (MFP) [42, 43], an indication of a crossover from ballistic into diffusive transport regimes [44, 45]. In fact, a theoretical work suggested that all experiments to date are actually carried out in the quasi-ballistic, rather than the diffusive regime [20]. Another recent theoretical study showed that in the case of pristine 1D channels the thermal conductivity could even increase with confinement [46], and it is even a function of the width-dependent phonon spectra [18]. References [47-49], demonstrated that the thermal conductivity in 1D channels grows as a power-law function of the length and that roughness affects the value of the exponent of this dependence.

The phonon spectrum of ultra-narrow GNRs and 1D-dimensional channels in general, however, consists of various phonon modes and polarizations, which react differently in the presence of disorder (e.g. line-edge roughness) and exhibit

different mean-free-paths and localization lengths. The few studies that attempt to address this issue (for different families of 1D channels) reach various and differing conclusions. A study on thermal transport in 1D Si nanowires, for example, indicated that line-edge roughness scattering affects the thermal conductivity by introducing band-mismatch in the optical region of the spectrum [14]. Different works attribute the reduction in thermal conductance to phonon localization and the appearance of non-propagating modes [13, 50, 51]. Specifically in the case of GNRs, it is indicated that the majority of eigenmodes are localized and do not contribute to thermal transport [52], whereas other studies suggest that heat transport is semi-ballistic [45]. Most studies, however, examine and present how the overall thermal conductivity (or thermal conductance) behaves under disorder, and dimensionality scaling. On the other hand, a lot of information about what determines the overall phonon transport properties resides in the individual phonon frequencies in the phonon spectrum. Thus, a study on how line edge disorder in 1D GNR channels affects phonon modes of different frequencies and wavevectors in the entire phonon spectrum will be extremely helpful in providing insight in thermal transport at low-dimensions.

In this work we theoretically investigate the effect of line edge roughness and confinement in phonon transport in ultra-narrow GNRs for the modes in the entire energy spectrum independently. The basic conclusions of this study can be applied generically to other 1D systems. Four distinct behaviors within the phonon spectrum in the presence of disorder are identified: i) the low-energy, low-wavevector acoustic branches are affected the least by edge disorder; ii) energy regions that consist of a dense population of relatively 'flat' phonon modes (including the optical branches) are also not significantly affected; iii) 'quasi-acoustic' bands that lie within the intermediate region of the spectrum are strongly affected by disorder; iv) the strongest reduction in phonon transmission is observed in energy regions that are composed of a small density of phonon modes. In this case, we describe a new effect, namely the creation of effective 'transport gaps' in the phonon spectrum as a result of band-mismatch in the presence of roughness, which drives transport strongly into the localization regime. We then show that the dependence of the thermal transport properties on the length and the width and the channel can be characterised by specific exponents in the form of L^{α}, and W^{β}, which indicate the dominant transport regimes from semi-ballistic to localization. The length dependence exponent for the ultra-narrow channels examined is in agreement with results in wider, but longer channels, as well, whereas the width dependence exponent is another new result we present, which is only studied expensively in the case of electrons for such ultra-narrow channels, but not phonons.

II. METHODS

We employ the NEGF method, which can take into account the exact geometry of the roughness without any underlying assumptions, while we describe the phonon spectrum atomistically using the force constant method (FCM). The NEGF method is appropriate for studies of phonon transport in geometries with disorder because the exact geometry is included in the construction of the dynamical matrix. Employing an atomistic approach that considers the discrete nature of the line-edge roughness and accurately models its impact on phonon modes is essential for the analysis of thermal properties of narrow GNRs (with W<20nm). In addition, this approach allows the description of channels with 100s of thousands of atoms, something that would be computationally extremely difficult to implement using *ab initio* DFT methods, for example. The method considers the wave nature of phonons, rather than their particle description, and all interference and localization effects, which could be important in low-dimensional channels, are captured. In addition, it is most appropriate for the purposes of this study, which investigates the influence of line-edge roughness for phonons of different frequencies of the spectrum, as NEGF computes the energy resolved phonon transmission function. The system geometry consists of two semi-infinite contacts made of pristine GNRs, surrounding the channel in which we introduce line-edge roughness. The Green's function is given by:

$$G(E)=\left[E^2 I - D - \Sigma_1 - \Sigma_2\right]^{-1} \tag{1}$$

where D is device dynamical matrix and $E=\hbar\omega$ is the phonon energy. The contact self- energy matrices $_{1,2}$ are calculated using the Sancho-Rubio iterative scheme. The transmission probability through the channel can be obtained using the relation:

$$T_{\mathrm{ph}}(\omega)=Trace\left[\Gamma_1 G \Gamma_2 G^{+}\right] \tag{2}$$

where $_1$ and $_2$ are the broadening functions of the two contacts defined as $\Gamma_{1,2}=i\left[\Sigma_{1,2}-\Sigma_{1,2}^{+}\right]$. The thermal conductance can then be calculated in the framework of the Landauer formalism as:

$$K_1=\frac{1}{2\pi\hbar}\int_0^{\infty} T_{\mathrm{ph}}(\omega)\hbar\omega\left(\frac{\partial n(\omega)}{\partial T}\right)d(\hbar\omega) \tag{3}$$

where $n(\omega)$ is the Bose-Einstein distribution and T is the temperature. In this work we consider room temperature T=300K. At room temperature and under ballistic conditions the function inside the integral spans the entire energy spectrum [53, 46], which allows phonons of all energies to contribute to the thermal conductance.

Under the harmonic approximation, the motion of atoms can be described by a dynamical matrix as:

$$D=[D_{3\times 3}^{(ij)}]=\left[\frac{1}{\sqrt{M_i M_j}}\begin{cases} D_{ij} & i\neq j \\ -\sum_{l\neq i} D_{il} & i=j \end{cases}\right] \tag{4}$$

where $M_{i,j}$ is the atomic mass of the i^{th}, j^{th} carbon atom (in this case all atoms have the same mass), and the dynamical matrix component between atoms 'i' and 'j' is given by:

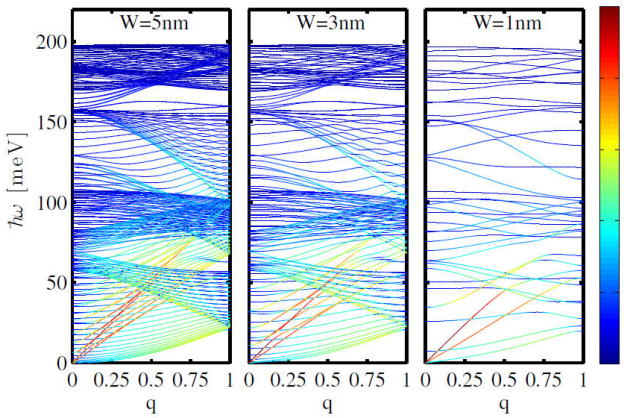

Fig. 1. Typical phonon dispersions for GNRs [55]. (a) *W*=5nm, (b) *W*=3nm, (c) *W*=1nm wide GNRs. As the width is decreased, the number of phonon modes is reduced. The colormap shows the contribution of each phonon state to the total thermal conductance (red: largest contribution, blue: smallest contribution).

$$D_{ij} = \begin{bmatrix} D_{xx}^{ij} & D_{xy}^{ij} & D_{xz}^{ij} \\ D_{yx}^{ij} & D_{yy}^{ij} & D_{yz}^{ij} \\ D_{zx}^{ij} & D_{zy}^{ij} & D_{zz}^{ij} \end{bmatrix} \tag{5}$$

where

$$D_{mn}^{ij} = \frac{\partial^2 U}{\partial r_m^i \partial r_n^j}, \quad i, j \in N_A \text{ and } \quad m, n \in [x, y, z] \tag{6}$$

is the second derivative of the potential energy (U) after atoms '*i*' and '*j*' are slightly displaced along the *m*-axis and the *n*-axis (∂r_m^i and ∂r_n^j), respectively.

For setting up the dynamical matrix component between the i^{th} and the j^{th} carbon atoms, which are the N^{th} nearest-neighbors of each other, we use the force constant method (FCM), involving interactions up to the fourth nearest-neighbor [54, 55]. The force constant tensor is given by:

$$K_0^{(ij)} = \begin{bmatrix} \phi_r^{(N)} & 0 & 0 \\ 0 & \phi_{ti}^{(N)} & 0 \\ 0 & 0 & \phi_{to}^{(N)} \end{bmatrix} \tag{7}$$

where $\phi_r^{(N)}$, $\phi_{ti}^{(N)}$, and $\phi_{to}^{(N)}$ are the radial, the in-plane transverse, and the out-of-plane transverse components respectively. The force constant fitting parameters are taken from Ref. [56] and are shown to accurately reproduce the phonon dispersion of graphene. The 3x3 components of the dynamical matrix are then computed as:

$$D_{ij} = U_m^{-1} K_0^{(ij)} U_m \tag{8}$$

where U_m is a unitary rotation matrix defined as:

$$U_m = \begin{bmatrix} \cos\theta_{ij} & \sin\theta_{ij} & 0 \\ -\sin\theta_{ij} & \cos\theta_{ij} & 0 \\ 0 & 0 & 1 \end{bmatrix} \tag{9}$$

Assuming the graphene sheet is located in the *x*-*y* plane, θ_{ij} represents the angle between the *x*-axes and the bond between the i^{th} and j^{th} carbon atom.

In addition, the phonon dispersion can be computed by solving the following eigenvalue problem using a unit cell:

$$\left[D + \sum_l D_l \exp\left(i\vec{q}.\Delta\vec{R}\right) \right] \psi(\vec{q}) = \omega^2(\vec{q})\psi(\vec{q}) \tag{10}$$

where D_l is the dynamical matrix representing the interaction between the cell and its neighboring cells spaced by $\Delta\vec{R}$, and $\psi(\vec{q})$ is the phonon mode eigenfunction at wavevector $\vec{q}$.

III. The Influnce of Confinement

Figures 1a, 1b, and 1c show typical dispersion relations for GNR channels of widths *W*=5nm, *W*=3nm, and *W*=1nm, respectively [55]. The *W*=1nm case resembles a purely 1D channel, whereas at a width of *W*=5nm the dispersion diverts towards 2D (although the dispersions in both cases are 1D). These sizes are computationally manageable, and comparison between their transport properties allows comparison between 1D and less confined, 'towards 2D', phonon transport. The colormap in Fig. 1 shows the contribution of each phonon state to the ballistic thermal conductance at *T*=300K [55]. To analyze the observed features of the GNR phonon dispersions, we first discuss the graphene phonon dispersion. In graphene, there are 6 phonon modes, 3 acoustic and 3 optical modes [56]. The highest frequency acoustic mode is the longitudinal acoustic (LA) mode, the next one is the in-plane transverse acoustic mode (TA) and lowest frequency mode is the out-of plane acoustic mode (ZA). The latter is recently shown to make the largest contribution to the thermal conductivity of graphene [57]. The highest frequency optical mode is the longitudinal optical (LO), followed by the in-plane transverse optical (TO), and the lowest is the out-of-plane optical (ZO) [58]. The LA mode of the GNRs shown in Fig. 1 is the corresponding LA mode of graphene with group velocity v_s=19.8 km/s. The LA and TA modes are linear at low frequencies, and extend up to *E*~0.16eV and *E*~0.14eV, respectively. The ZA mode is quadratic for low frequencies and extends up to *E*~0.07eV. At the higher part of their energy region, the acoustic modes become relatively 'flat'. The ZO modes extend from *E*~0.7eV-0.11eV, whereas the LO and TO modes are located at higher energies, from *E*~0.16eV-0.2eV. The relatively 'flat' mode regions around energies *E*~0.07eV-0.11eV consist of ZO modes, in addition to the dispersive LA and TA modes. The less dispersive modes located from *E*~0.11eV-0.16eV are the 'flat' parts of the LA and TA modes.

Three main changes on the phonon bandstructure can be observed as the width is reduced, i.e. comparing Fig. 1a with Fig. 1c: i) The optical and 'quasi-acoustic' modes (folded acoustic branches of the host material) show strong confinement dependence. The number of modes depends on the number of atoms within the unit cell. As the width is reduced, the number of modes in these regions is also reduced. ii) The number of acoustic modes remains intact, and they carry a much larger portion of the heat (as indicated by their

red coloring in Fig. 1a and 1c), especially in the case of the narrower GNR. iii) Small bandgaps appear in some regions in the bandstructure, especially in regions around the interface between the 'flat' optical modes and the more dispersive 'quasi-acoustic' modes (primarily around E=0.16 eV, and secondly around E=0.11 eV, and E=0.07 eV). Large regions in the phononic (E,q) space, especially in the 'quasi-acoustic' band regions, become 'empty' of modes (sparse) where for rather extensive energy and momentum intervals no phonon states exist. As we show below, such regions are extremely more sensitive to disorder compare to the rather dense mode regions of the spectrum.

IV. The Influence of Line-Edge Roughness

Next, we then investigate phonon transport in these low-dimensional GNRs in the presence of disorder. At such small ribbon widths with rough edges, the edge-phonon scattering is the dominant scattering mechanism [15]. For this, we simulate rough GNR channels of width W=5nm (relatively wide) down to W=1nm (purely 1D), and examine the phonon transmission across the phonon energy spectrum as the length of the GNR increases even up to 1000 nm (i.e. as the effective disorder increases). To provide an indication of the computational cost, we note that the largest nanoribbon we consider, of width W=5nm and channel length of L=500nm, consists of nearly 100,000 atoms. To describe the motion of each atoms a 3×3 matrix is needed, see Eq. (4) and Eq. (5). The resulting Hamiltonian and Green's functions at each energy point are matrices with a size of 300,000×300,000. To simulate the phonon transmission of this structure, it takes several hours on a 16 core machine with 128 GB of memory. Since the roughness produces a random edge topology, all results we present, are extracted by averaging 50 different realizations of roughened channels. We note that in this work our goal was to investigate effects of disorder on the phonon transport of 1D channels. However, using the same computational resources we could scale the GNR width even up to W=50nm, but in that case we would have to reduce the length down to L=50nm-100nm. At such wide and short channel, though, the effects of edge roughness are minimized.

To construct the line-edge-roughness geometry on the edge of the GNR, we use an exponential autocorrelation function as explained in our previous work [59]. We construct a roughness line at the top and bottom edges of the GNR and atoms located in the outer direction of the lines are removed, whereas all regions in the inner part of the lines are filled with atoms if needed. In this work we only consider GNRs with armchair edges, however, we have also performed simulations for GNRs with zig-zag edges and we verify that the main conclusions of this work still apply to the zig-zag GNR case as well. Finally, we note that the GNRs are assumed to be suspended and the edge atoms are allowed to move freely, vibrating in harmony with the other atoms according to the lattice wave/dynamics.

Since each phonon mode responds differently to disorder, it is essential to investigate the regions of operation of the different modes, and identify the different behaviors, from semi-ballistic to localization. To illustrate the distinctly different behavior of the various phonon modes in the presence of line edge roughness, Fig. 2 shows the product of the transmission times the length of the channel (T_{ph}×L) versus channel length L at certain phonon frequencies as a function of the channel length L. In the case of ballistic transport, the T_{ph}×L product increases linearly. In the case of diffusive transport it remains constant. In the case of sub-diffusive transport the product reduces with length [60], and for localized transport, the product drops exponentially. We focus on four different phonon categories, and pick a specific phonon energy within the spectrum indicating each of these categories. These are: i) acoustic phonons (E=0.01eV) shown in Fig. 2a, ii) optical, 'flat' dispersion phonons (E=0.19eV) shown in Fig. 2b, iii) 'quasi-acoustic', dispersive phonon modes (E=0.13eV) shown in Fig. 2c, and iv) regions of very low mode densities, in which confinement can even result in narrow bandgaps (E=0.16eV) shown in Fig. 2d. In each figure we consider GNRs of widths W=5 nm (red-dashed lines) down to W=1 nm (blue lines).

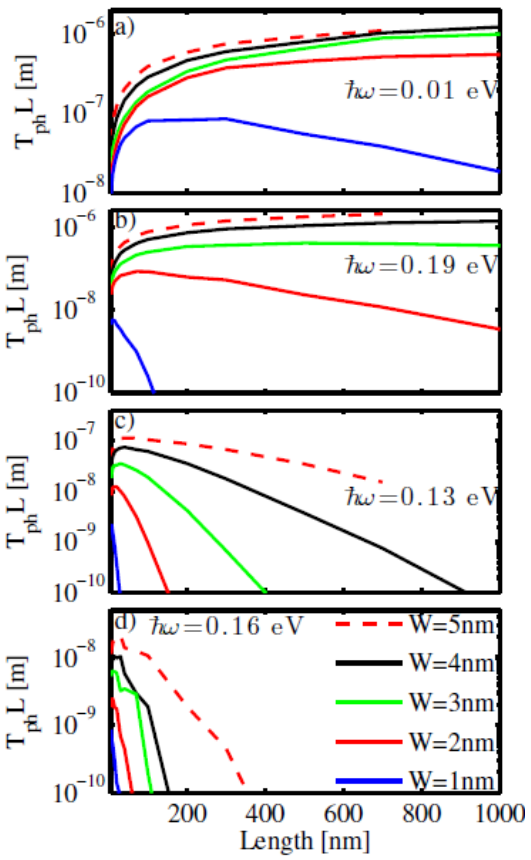

Fig. 2. The phonon transmission times the channel length (T_{ph}×L) versus channel length for rough nanoribbons at energies (a) E=0.01eV, which correspond to the acoustic branches, (b) E=0.19eV, which corresponds to the optical branches, (c) E=0.13eV, and (d) E=0.16eV. In each sub-figure, results for channels of width W=5nm (red-dashed lines) down to W=1nm (blue lines) are shown.

From Fig. 2a, it can be seen that for the wider GNR channels, the acoustic modes are ballistic, or semi-ballistic, even for channel widths W=3nm and lengths up to L=1μm. In the ultra-narrow W=1nm GNRs (blue line in Fig. 2a), the acoustic modes reach the diffusive regime at around lengths of

L~200nm, and get into the localized regime for lengths larger than L~700nm. The influence of roughness in the acoustic modes, in general, is relatively weak, and can be understood from the fact that they are composed of LA modes with long wavevectors [8, 10], which makes them very weakly affected by defects, and this is the case for both wider and ultra-narrow GNRs. Interestingly, a similar trend is observed for the optical modes (Fig. 2b) as well at energies E=0.19eV. GNRs with widths W=5nm (red-dashed line) and W=3nm (green line) indicate a semi-ballistic behavior even up to channel lengths of hundreds of nanometers. In the W=1nm and W=2nm cases, however, the optical modes reach the sub-diffusive and localization regimes at lengths even below L~100nm. Under such narrow channels, the optical modes density becomes sparse. This combined with the fact that the optical modes are rather 'flat', introduces band-mismatch from layer to layer along the transport path in the presence of line-edge roughness, which strongly degrades phonon transmission.

The behavior of the 'quasi-acoustic' modes at energies E=0.13eV (Fig. 2c), on the other hand, is very different. These modes enter the diffusive regime at much shorter channel lengths compared to the acoustic and the optical modes. They even enter the localization regime after L~300nm for the W=5nm GNRs, after L~100nm for the W=3nm GNRs, and just after L~10nm for the W=1nm GNRs. This is quite intriguing since these are dispersive modes with much higher group velocities compared to the optical modes. The strongest reduction in transmission, however, is observed for the energy regions E~0.16eV (Fig. 2d), which are regions of low mode density (see Fig. 1). For these modes, the transmission is diminished after channel lengths of L~200nm in the case of the wider channels, and after L~10nm in the case of the ultra-narrow channel.

The reason why the 'quasi-acoustic' mode regions and the low density mode regions behave so drastically different compared to the optical modes can be explained by their behavior under confinement. Figure 1 shows that under confinement, the number of modes in these energy regions (E~0.13, and E~0.16) is reduced significantly, making these regions look almost 'empty' of modes. In the presence of line edge roughness in a real geometry, the sparsity of the modes makes these particular energy regions more susceptible to the formation of 'effective' bandgaps by increasing the band-mismatch between the modes in the physical channel regions along the propagation path of the phonons. Such an event is not the case for the optical modes for the geometries we examine. The 'effective' transmission bandgap formation is demonstrated in the transmission functions shown in logarithmic scale in Fig. 3 for the W=5nm channel under ballistic (pristine channel) conditions (black-dashed line) and under line edge roughness when the channel length is L=5nm, 40nm, 100nm, and 500nm (black-solid line). For short channels, the transmission is not significantly disturbed. For the longer channels, however, it is evident that for energies around E~0.07eV and E~0.13eV large 'effective' bandgaps form as indicated by the arrows. Notice the even larger bandgap formation at energies E~0.16eV. Comparing this to Fig. 1c, there is a clear indication that the energy regions which become sparse of modes under confinement are very

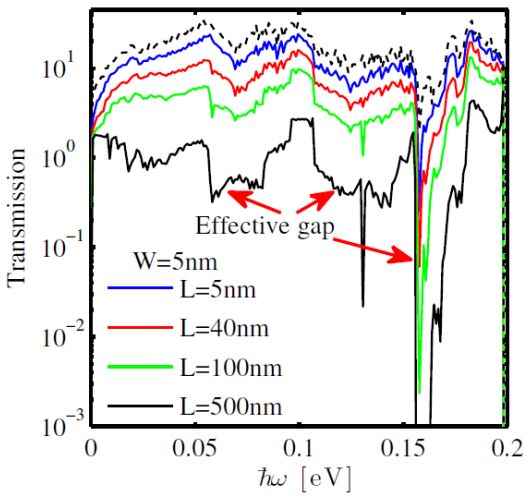

Fig. 3. The transmission function versus energy in logarithmic scale for rough edge GNRs of width W=5nm. The ballistic transmission (pristine GNRs, non-roughened ribbons) is depicted by the black-dashed line. Results for nanoribbons with lengths L=5nm (blue line), L=40nm (red line), L=100nm (green line), and L=500nm (black-solid line) are shown.

susceptible to roughness in less confined geometries as well. This suggests that the influence of confinement has similar features in the transmission as the effect of roughness.

The behavior described above should hold for any sparse mode energy regions. Note, for example, that gaps do not form in the regions of the 'flat' optical modes, and the transmission does not degrade as much. Under strong confinement, however, the 'flat' optical mode regions become sparser, and in extreme cases begin to 'look' like the low-density regions as well. Under these conditions, they could also be subject to band mismatch, and to the effect we describe above. In this context, the thermal conductivity is a function of the width-dependent phonon spectra [15], for which line edge roughness could either further increase the band mismatch, or form 'effective' transport bandgaps.

We would like to mention that the purpose of this work was to elucidate the main features of 1D transport of phonons in the presence of disorder in a general sense. An important message we convey in this work is the fact that just by looking at how the phonon bandstructure behaves under confinement, and its low-dimensional dispersion features, one can provide an indication of how the modes will behave under edge roughness. Qualitatively, the behavior we describe should hold for other low-dimensional materials beyond GNRs, but also be relevant to phonon dispersions extracted through other methods, e.g. DFT calculations etc. Another important point to make, is that the diffusive regime in our calculations is caused by edge roughness, and not phonon-phonon interactions, which are not included in the simulations. Including the full unharmonicity of the material within NEGF would have been a much more computationally intensive effort. However, edge roughness under ultra-narrow channels could have a much stronger effect compared to phonon-phonon interactions and the thermal conductance could reach diffusive, even

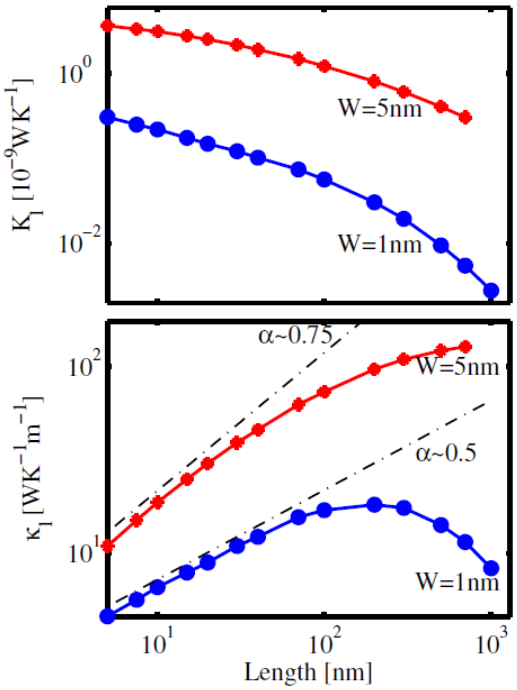

Fig. 4. The thermal conductance (a) and conductivity (b) versus channel length for GNRs with widths W=5nm (red-diamond) and W=1nm (blue-circles).

localization behavior even before phonon-phonon interaction becomes important. This depends on how smaller the MFP of edge disorder is compared to the MFP of phonon-phonon interaction (which is in the 100 of nanometers in graphene).

Graphene and graphene nanoribbons indicate significant anisotropic behavior and the type of edges plays a role. The chirality of GNRs, i.e. armchair (AGNRs), or zig-zag (ZGNRs) can provide anisotropy in phonon transport behavior (although smaller compared to electronic transport anisotropy). In Ref. [61], for example, using the phonon Boltzmann transport equation, it was shown that the amount of anisotropy between AGNR and ZGNR ribbons can be significant, which also increases as the ribbon width decreases and as the roughness amplitude increases. We have performed the same simulations for the zig-zag GNRs (ZGNRs), in addition to the armchair GNRs we present in this work. The results for ZGNRs are very similar to those for AGNRs, with somewhat less distinctive, but still strong reductions being observed in the transmission function around E=0.07eV, E=0.11eV and E=0.16eV. The phonon spectrum of ZGNRs has slightly more dispersive bands, something also validated by first principle calculations [28]. This makes their ballistic thermal conductance and transmission somewhat higher compared to AGNRs and does not allow the formation of 'effective bandgaps' upon confinement and roughness as easily. The main qualitative trends, however as in the case of AGNRs are also observed for ZGNRs.

We next analyse how these features show up and affect the overall thermal *conductivity* of ultra-narrow 1D GNR channels. The thermal conductivity of the GNR channels is a length dependent quantity and calculated using the thermal conductance as $\kappa_l = LK_l / A$, where A is the cross section area of the GNR with its height assumed to be 0.335nm. Figure 4a shows the thermal conductance, K_l, versus channel length for GNRs with width W=5nm (red-diamond line) and W=1nm (blue-circle line). The thermal conductance drops as the channel length increases, and it is significantly lower in the case of the narrower channel with W=1nm, compared to the wider channel of W=5nm. Figure 4b shows the extracted thermal conductivity, κ_l. Since the dominant mean-free-paths for scattering can be quite large, the thermal conductivity will increase with an increase in the channel length, until the channel length extends beyond the dominant phonon mean-free-paths. These are the mean-free-paths of the acoustic low-energy phonons (see Fig. 2a), which can extend even up to several micrometers (in some cases even up to millimeters). Thus, ballistic transport dictates that the thermal conductivity increases linearly with channel length, while saturation comes due to scattering. The increase in thermal conductivity with channel length for short channels, and saturation for the longer ones, indicates the transition between ballistic and diffusive transport which was also observed at various instances [45, 62]. For the wider GNR channel with W=5nm, the saturation begins for length scales of several hundreds of nanometers. Other theoretical studies also suggest the $\langle \lambda \rangle \sim 600nm$ for the phonon-phonon interactions-caused MFP in graphene and carbon nanotubes, but this should not be confused with the edge-disorder-caused MFP [63-66]. At this channel length, however, the narrower GNR with W=1nm is already driven into the sub-diffusive and even into the localization regime, where the conductivity reduces with increasing the length of the channel (blue line). In general, however, it is expected that if phonon-phonon scattering was considered, the diffusive regime would have been reached at somewhat shorted channel lengths, and the effects of localization would have been somewhat smoothened. We note that a more detailed description of the extraction of the MFPs, the localization lengths, as well as theoretical validation of phonon localization, can be found in our previous work in Ref. [55].

An important parameter that characterizes the heat transport properties of the material and the strength of the line-edge roughness, is the slope of the thermal conductivity versus length in the semi-ballistic regime (left side of Fig. 4b). The dashed-dotted lines in Fig. 4b indicate the slopes in the two channels. Unity slope would be expected for purely ballistic channels. The strength of the line edge roughness is indicated by the deviation from unity for short channel lengths [67, 68]. A power law behavior L^{α} is expected for 1D channels [67, 68]. From our data in Fig. 4, the wider channel with W=5nm has α=0.7. As the width decreases to W=1nm, the exponent is reduced to α=0.5, indicating the stronger influence of line-edge roughness on the narrower channel [55].

Another important aspect of the thermal conductivity in ultra-narrow channels under the influence of line-edge roughness is the trend of the thermal conductivity versus the *width* of the channel. This has in the past raised significant

attention in the case of electronic transport in low-dimensional channels, dominated by surface roughness scattering [69]. In the case of electronic transport, the surface roughness scattering limited electronic mobility or conductivity of a semiconductor channel follows a D^6 trend, where D is the diameter of the channel, or the confinement width in the case of 2D channels [70, 71]. Thus, as the confining dimension is reduced, the transport properties degrade rapidly. In silicon channels for example, this effect becomes dominant at confinement length scales below 10nm. This trend originates from how the subbands of the material shift in energy upon quantization, and how that determines the surface roughness scattering matrix element.

In the case of phonon transport, on the other hand, it is not clear how the thermal conductivity of a roughened low-dimensional channel will behave as a function of its width. The reason is that in the case of phonons, the lowest energy bands, i.e. the acoustic modes always start from zero energy and are not affected by confinement. As we show below, however, such information for phonons would also provide understanding on which phonon transport regime the channel operates at. Figure 5 shows the calculation of the thermal conductance in the roughened GNR channels for two different lengths versus their width. We examine a very short channel, of length L_{ch}=5nm (red line), and a longer channel of length L_{ch}=500nm (blue line). The widths we consider vary from ultra-narrow W=1nm up to W=5nm. The dashed lines indicate a fitting of the thermal conductance simulation points using a function W^{β}.

It is clearly observed that the thermal conductance is channel length and width dependent. Here, we discuss the behavior under three different transport regimes in Fig. 5: i) the ballistic regime, ii) the diffusive regime, and iii) the localization regime. The very short channel with L_{ch}=5nm (red line), falls into the semi-ballistic transport regime, as also shown by the linear increases of the conductivity in Fig. 4 (left side), and the conductance can be fitted by a single function with a single exponent β=1.46, as $W^{1.46}$. A purely ballistic channel would exhibit W^1 as the thermal conductance increases linearly with the width of the GNR due to the linear increase in the number of conducting phonon modes with channel width. The slightly larger exponent than unity indicates that the strength of the line-edge roughness weakens as the width increases. For the longer channel L_{ch}=500nm (blue line), clearly two different regions can be identified. The wider channels, which fall into the super-diffusive towards diffusive transport regime, as can be observed in Fig. 4b (flattened right side of the red line for W=5nm), can be described by an exponent β=2, i.e. W^2. In the case of the ultra-narrow W=1nm, L_{ch}=500nm channels (left side of the blue line in Fig. 5), however, the exponent β=2 cannot describe the data. In contrast, a larger exponent β=2.9, i.e. $W^{2.9}$, provides a better fit. This is a clear indication that the channel falls in a regime beyond diffusion, more closer to localization, as also observed in Fig. 4b (right side of the blue line, for W=1nm). Thus, the important observation from Fig. 5 is that we can

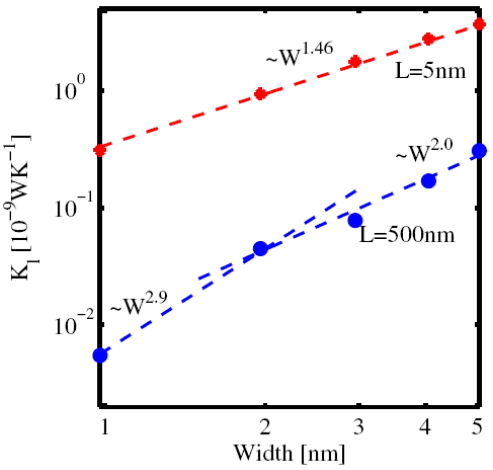

Fig. 5. The thermal conductance versus channel width for GNRs with lengths L=5nm (red-diamonds) and L=500nm (blue-circles). Characteristic exponents in the form W^{β} are indicated.

map the roughened channel transport behavior by the dependence of the conductance on the channel width. In the cases we have studied, it seems that exponents from β=1 to β=2 indicate semi-ballistic to diffusive transport, whereas exponents around and above β=3 indicate localization.

Thus, extracting characteristic exponents based on the geometry of the system, could serve as a guide to experiments to elucidate the transport regime of operation. Phonon localization, in particular, is a transport regime which dominates the flow of phonons in low dimensional channels. Loh *et* al. [72] studied the influence of vacancies in phonon transport in graphene and showed that acoustic modes tend to get localized around the vacancies, which results in a large reduction in the thermal conductivity. Isotope scattering could also cause localization of high energy optical phonon modes in graphene [73]. Kim *et* al. have recently also experimentally showed that phonon localization appears in graphene in the presence of graphene nanobubbles formed by noble gas atom implantation [74]. Wang *et* al. [10] showed that the anisotropic behavior of thermal conductivity between zigzag and armchair edge graphene nanoribbons originates from the stronger localization around the armchair edges. In a different work, Jiang *et* al. studied phonon transport in 'kinked' edge silicon nanowires (edges in a zig-zag form), and demonstrated that the twisting and transverse phonon modes also suffer localization and reduce heat transport [75]. Of course, localization is a coherent process, and inelastic scattering introduces decoherence, which could diminish localization. As Loh *et* al. compute, this can be the case for optical phonons in graphene, but not for acoustic modes due to larger inelastic mean-free-paths for scattering compared to localization lengths [72]. Since acoustic modes are the dominant heat carriers, the presence of disorder caused localization will have dramatic reduction in thermal transport.

Finally, we note that although we consider suspended GNRs, our general conclusions would be valid for GNRs

placed on substrates as well. Placing GNRs a substrate introduces an additional scattering effect, namely substrate scattering, as described by Aksamija *et* al in Ref. [23]. In that work, using Monte Carlo simulations for phonons in large area GNRs suspended on SiO_2 were carried out. The substrate scattering was modeled as a point interaction with small patches where the ribbon is in contact with the substrate [76]. The authors have shown that indeed substrate scattering is a dominant scattering mechanism, but the mean-free-path (MFP) of substrate scattering is about 67nm, and it dominates phonon transport for GNRs with widths larger than 1μm. For narrow GNRs with widths below W=130nm (the GNRs we investigate here are even smaller down to a few nanometers), line-edge roughness dominates phonon transport. In any case, for substrate scattering to be modelled within NEGF, one should construct a dynamical matrix that could account for the deviation in bond length and angle. This should not be based on the Force Constant Method (in which case the parameters are constant), but potentially based on first principle calculations or valence force fields, in which the potential energy and force constants are calculated for each atom based on its own position and the position of its neighbors. These methods require much larger computational time, in contrast to the FCM, however. The NEGF formalism could then be employed using that dynamical matrix.

V. Conclusions

In conclusion, we have investigated the thermal transport properties of low-dimensional, ultra-narrow graphene nanoribbon (GNR) channels under the influence of line-edge roughness disorder. We employed the non-equilibrium Green's function (NEGF) method for phonon transport and the force constant method for the description of the phonon modes. We show that the effect of line edge roughness affects different parts of the spectrum in different ways: i) Disorder does not significantly affect the low frequency acoustic modes significantly, except under extreme confinement in purely 1D channels; ii) Disorder is not very detrimental for regions of the spectrum with a dense population of modes such as the optical modes either; iii) Regions of the spectrum with low mode density end up becoming 'effective' transport gaps as the length of the channel increases, or the width decreases, and contribute little to thermal transport; iv) Regions of the spectrum with very low mode densities, populated with relatively 'flat' modes suffer from band mismatch in the presence of both confinement or roughness, which reduces their ability to carry heat. In situations (iii) and (iv) transport is driven into the localization regime. We show that the dependence of the channel transport properties (conductivity and conductance) versus length and versus width could indicate the transport regime under which heat propagates through the channel. Our results present generic features of 1D phonon transport, and could be relevant to different nanochannels as well.

Acknowledgment

The authors acknowledge Dr. Mahdi Pourfath, Dr. Hans Kosina, and Dr Mischa Thesberg for helpful discussions.

References

[1] D. L. Nika, A. S. Askerov, and A. A. Balandin, "Anomalous size dependence of the thermal conductivity of graphene ribbons," Nano Lett., 12, pp. 3238-3244, 2012.

[2] N. Mingo, D. A. Broido, "Length dependence of carbon nanotube thermal conductivity and the "problem of long waves"," Nano Lett., 5, pp. 1221-1225, 2005.

[3] L. Lindsay, D. A. Broido, and N. Mingo, "Lattice thermal conductivity of single-walled carbon nanotubes: Beyond the relaxation time approximation and phonon-phonon scattering selection rules," Phys. Rev. B, 80, 125407, 2009.

[4] L. Lindsay, D. A. Broido, and N. Mingo, "Flexural phonons and thermal transport in graphene," Phys. Rev. B, 82, 15427, 2010.

[5] D. L. Nika and A. A. Balandin, "Two-dimensional phonon transport in graphene," J. Phys.: Condens. Matter, 24, 233203, 2012.

[6] A. Balandin, "Thermal properties of graphene and nanostructured carbon materials," Nat. Materials,10, p. 569, 2011.

[7] A. V. Savin and Y. S. Kivshar "Vibrational Tamm states at the edges of graphene nanoribbons," Phys. Rev. B, 81, 165418, 2010.

[8] Z. Aksamija and I. Knezevic, "Lattice thermal transport in large-area polycrystalline graphene," Phys. Rev. B., 90, 035419, 2014.

[9] H. Karamitaheri, N. Neophytou, M. Pourfath, R. Faez, and H. Kosina, "Engineering Enhanced Thermoelectric Properties in Zigzag Graphene Nanoribbons," J. Appl. Phys., 111, 054501, 2012.

[10] Y. Wang, B. Qiu, and X. Ruan, "Edge effect on thermal transport in graphene nanoribbons: A phonon localization mechanism beyond edge roughness scattering," Appl. Phys. Lett., 101, 013101, 2012.

[11] F. Mazzamuto, J. Saint-Martin, A. Valentin, C. Chassat, and P. Dollfus, "Edge shape effect on vibrational modes in graphene nanoribbons: A numerical study," J Appl. Phys., 109, 064516, 2011.

[12] Z. W. Tan, J.-S. Wang, and C. K. Gan, "First-principles study of heat transport properties of graphene nanoribbons," Nano Lett., 11, pp. 214–219, 2011.

[13] D. Donadio and G. Galli, "Atomistic Simulations of Heat Transport in Silicon Nanowires," Phys. Rev. Lett. 102, 195901, 2009.

[14] M. Luisier, "Investigation of thermal transport degradation in rough Si nanowires," J. Appl. Phys., 110, p. 074510, 2011.

[15] W. J. Evans, L. Hu, and P. Keblinski, "Thermal conductivity of graphene ribbons from equilibrium molecular dynamics: Effect of ribbon width, edge roughness, and hydrogen termination," Appl. Phys. Lett., 96, 203112, 2010.

[16] A. Hochbaum, R. Chen, R. Delgado, W. Liang, E. Garnett, M. Najarian, A. Majumdar, and P. Yang, "Enhanced thermoelectric efficiency of rough silicon nanowires," Nature, 451, 163, 2008.

[17] A. I. Boukai, Y. Bunimovich, J. Tahir-Kheli, J.-K. Yu, W. A. Goddard, and J. R. Heath, "Silicon nanowires as efficient thermoelectric materials," Nature, vol. 451, pp. 167-171, 2008.

[18] W. J. Evans, L. Hu, and P. Keblinski, "Thermal conductivity of graphene ribbons from equilibrium molecular dynamics: Effect of ribbon width, edge roughness, and hydrogen termination," Appl. Phys. Lett., 96, 203112, 2010.

[19] K. Termentzidis, T. Barreteau, Y. Ni, S. Merabia, X. Zianni, Y. Chalopin, P. Chantrenne, and S. Voltz, "Modulated SiC nanowires: Molecular dynamics study of their thermal properties," Phys. Rev. B, 87, 125410, 2013.

[20] Claudio Melis and Luciano Colombo, "Lattice Thermal Conductivity of $Si_{1-x}Ge_x$ Nanocomposites," Phys. Rev. Lett., 112, 065901, 2014.

[21] D. Donadio, and G. Galli, "Temperature Dependence of the Thermal Conductivity of Thin Silicon Nanowires," Nano Lett., 10, 847-851, 2010.

[22] Z. G. Fthenakis, Z. Zhu, and David Tomanek, "Effect of structural defects on the thermal conductivity of graphene: From point to line defects to haeckelites," Phys. Rev. B, 89, 125421, 2014.

[23] Z. Aksamija and I. Knezevic, "Thermal transport in graphene nanoribbons supported on SiO_2," Phys. Rev. B, 86, 165426, 2012.

[24] S. Wolf, N. Neophytou, and H. Kosina, "Thermal conductivity of silicon nanomeshes: Effects of porosity and roughness," J. Appl. Phys., 115, 204306, 2014.

[25] M. Maldovan, "Thermal conductivity of semiconductor nanowires from micro to nano length scales," J. Appl. Phys., 111, 024311, 2012.

[26] A. J. H. McGaughey and M. Kaviany, "Quantitative validation of the Boltzmann transport equation phonon thermal conductivity model under the single-mode relaxation time approximation," Phys. Rev. B, 69, 094303, 2004.

[27] H. Karamitaheri, N. Neophytou, M. Pourfath, R. Faez, and H. Kosina, "Engineering enhanced thermoelectric properties in zigzag graphene nanoribbons," J. Appl. Phys., 111, 054501, 2012.

[28] Z. W. Tan, J.-S. Wang, and C. K. Gan, "First-Principles Study of Heat Transport Properties of Graphene Nanoribbons," Nano Lett., 11, 214–219, 2011.

[29] M. Luisier, "Investigation of thermal transport degradation in rough Si nanowires," J. Appl. Phys., 110, 074510, 2011.

[30] Z. Huang, T. S. Fisher, and J. Y. Murthy, "Simulation of thermal conductance across dimensionally mismatched graphene interfaces," J. Appl. Phys., 108, 114310, 2010.

[31] Y. Xu, J.-S. Wang, W. Duan, B.-L. Gu, and B. Li, "Nonequilibrium Green's function method for phonon-phonon interactions and ballistic-diffusive thermal transport," Phys. Rev. B, 78, 224303, 2008.

[32] T. Yamamoto and K. Watanabe, "Nonequilibrium Green's Function Approach to Phonon Transport in Defective Carbon Nanotubes," Phys. Rev. Lett., 96, 255503, 2006.

[33] N. Mingo, "Anharmonic phonon flow through molecular-sized junctions," Phys. Rev. B, 74, 125402, 2006.

[34] T. Markussen, "Surface Disordered Ge–Si Core–Shell Nanowires as Efficient Thermoelectric Materials," Nano Lett., 12, 4698-4704, 2012.

[35] C. Jeong, S. Datta, and M. Lundstrom, "Thermal conductivity of bulk and thin-film silicon: A Landauer approach," J. Appl. Phys., 111, 093708, 2012.

[36] L. G. C. Rego and G. Kirczenow, "Quantized Thermal Conductance of Dielectric Quantum Wires," Phys. Rev. Lett., 81, 232 1998.

[37] Y.-C. Wen, C.-L. Hsieh, K.-H. Lin, H.-P. Chen, S.-C. Chin, C.-L. Hsiao, Y.-T. Lin, C.-S. Chang, Y.-C. Chang, L.-W. Tu, and C.-K. Sun, "Specular Scattering Probability of Acoustic Phonons in Atomically Flat Interfaces," Phys. Rev. Lett., 103, 264301 2009.

[38] S. L. Broschat and E. I. Thorsos, "An investigation of the small slope approximation for scattering from rough surfaces. Part II. Numerical studies," J. Acoust. Soc. Am., 101, 2615-2625 , 1997.

[39] C. W. Chang, D. Okawa, H. Garcia, A. Majumdar, and A. Zettl, "Breakdown of Fourier's Law in Nanotube Thermal Conductors," Phys. Rev. Lett., 101, 075903, 2008.

[40] X. Ni, M. L. Leek, J.-S. Wang, and Y. P. Feng, B. Li, "Anomalous thermal transport in disordered harmonic chains and carbon nanotubes," Phys. Rev. B, 83, 045408, 2011.

[41] M. Wang, N. Yang, and Z.-Y. Guo, "Non-Fourier heat conductions in nanomaterials," J. Appl. Phys., 110, 064310, 2011.

[42] D. Singh, J. Y. Murthy, and T. S. Fisher, "On the accuracy of classical and long wavelength approximations forphonon transport in graphene," J. Appl. Phys., 110, 113510, 2011.

[43] Z. Xu et al, "Length-dependent thermal conductivity in suspended single-layer graphene", Nat. Comm., 5, 3679, 2014.

[44] S. Ghosh, W. Bao, D. L. Nika, S. Subrina, E. P. Pokatilov, C. N. Lau, and A. A. Balandin, "Dimensional crossover of thermal transport in few-layer graphene," Nature Materials, 9, 555-558, 2010.

[45] M. Bae, Z. Li, Z. Aksamija, P. N. Martin, F. Xiong, Z. Ong, I. Knezevic, and E. Pop, "Ballistic to diffusive crossover of heat flow in graphene ribbons," Nat. Comm. 4, 1734, 2013.

[46] H. Karamitaheri, N. Neophytou, and H. Kosina, "Anomalous diameter dependence of thermal transport in ultra-narrow Si nanowires," J. Appl. Phys., 115, 024302, 2014.

[47] S. Lepri, R. Livi, and Antonio Politi, "Heat Conduction in Chains of Nonlinear Oscillators," Phys. Rev. Lett., 78, 3996, 1997.

[48] B. Li and J. Wang, "Anomalous Heat Conduction and Anomalous Diffusion in One-Dimensional Systems," Phys. Rev. Lett., 91, 044301, 2003.

[49] G. Wu and J. Dong, "Anomalous heat conduction in a carbon nanowire: Molecular dynamics calculations," Phys. Rev. B, 71, 115410, 2005.

[50] Y. He, D. Donadio, and G. Galli, "Morphology and Temperature Dependence of the Thermal Conductivity of Nanoporous SiGe," Nano Letters, 11, 3608, 2011.

[51] R. Venkatasubramanian, "Lattice thermal conductivity reduction and phonon localizationlike behavior in superlattice structures," Phys. Rev. B,. 61, 3091-3097, 2000.

[52] A. V. Savin, Y. S. Kivshar, and B. Hu, "Suppression of thermal conductivity in graphene nanoribbons with rough edges," Phys. Rev. B, 82, 195422, 2010.

[53] T. Markussen, A.-P. Jauho, and M. Brandbyge, "Heat Conductance Is Strongly Anisotropic for Pristine Silicon Nanowires," Nano Lett., 8, 3771, 2008.

[54] H. Karamitaheri, N. Neophytou, M. Pourfath, and H. Kosina, "Study of Thermal Properties of Graphene-Based Structures using the Force Constant Method," J. of Computational Electronics, 11, 1, 14-21, 2012.

[55] H. Karamitaheri, M. Pourfath, H. Kosina, and N. Neophytou, "Low-dimensional phonon transport effects in ultra-narrow, disordered graphene nanoribbons," Phys. Rev. B, 91, 165410, 2015.

[56] R. Saito, M. Dresselhaus, G. Dresselhaus, "Physical Properties of Carbon Nanotubes," Imperial College Press, London, 1998.

[57] L. Lindsay, W. Li, J. Carrete, N. Mingo, D. A. Broido, and T. L. Reinecke, "Enhanced thermal conductivity and isotope effect in single-layer hexagonal boron nitride," Phys. Rev. B, 89, 155426, 2014.

[58] E. Pop, V. Varshney, and A. K. Roy, "Thermal properties of graphene: Fundamentals and applications," MRS Bulletin, 37, pp. 1273-1281, 2012.

[59] H. Karamitaheri, M. Pourfath, R. Faez, and H. Kosina, "Atomistic Study of the Lattice Thermal Conductivity of Rough Graphene Nanoribbons," IEEE Transactions on Electron Devices, 60, 7, 2142, 2013.

[60] B. Vermeersch, A. M. S. Mohammed, G. Pernot, Y.-R. Koh, and A. Shakouri, "Supperdiffusive heat conduction in semiconductor alloys. II. Truncated Levy formalism for experimental analysis," Phys. Rev. B, vol. 91, p. 085203, 2015.

[61] Z. Aksamija and I. Knezevic, "Lattice thermal conductivity of graphene nanoribbons: Anisotropy and edge roughness scattering," Appl. Phys. Lett., 98, 141919, 2011.

[62] J. Lee, J. Lim, and P. Yang, "Ballistic Phonon Transport in Holey Silicon," Nano Lett., 15, pp. 3273–3279, 2015.

[63] S. Ghosh, I. Calizo, D. Teweldebrhan, E. P. Pokatilov, D. L. Nika, A. A. Balandin, W. Bao, F. Miao, and C. N. Lau, "Extremely high thermal conductivity of graphene: Prospects for thermal management applications in nanoelectronic circuits," Appl. Phys. Lett., 92, 151911, 2008.

[64] E. Munoz, J. Lu, and B. I. Yakobson, "Ballistic Thermal Conductance of Graphene Ribbons," Nano Lett., 10, 1652, 2010.

[65] S. P. Hepplestone and G. P. Srivastava, "Low-temperature mean-free path of phonons in carbon nanotubes," J. Phys. Conf. Ser., 92, 012076, 2007.

[66] J. W. Che, T. Cagin, and W. A. Goddard, "Thermal conductivity of carbon nanotubes," Nanotechnology, 11, 65, 2000.

[67] Z. Guo, D. Zhang, and X.-G. Gong, "Thermal conductivity of graphene nanoribbons," Appl. Phys. Lett., 95, 163103, 2009.

[68] M. Park, S.C. Lee, and Y. S. Kim, "Length-dependent lattice thermal conductivity of graphene and its macroscopic limit," J. Appl. Phys., 114, 053506, 2013.

[69] E. Pop, "Energy Dissipation and Transport in Nanoscale Devices," Nano Research, 3, pp. 147-169, 2010.

[70] S. Jin, M. V. Fischetti, and T.-W. Tang, "Modeling of electron mobility in gated silicon nanowires at room temperature: Surface roughness scattering, dielectric screening, and band nonparabolicity," J. Appl. Phys., 102, 083715, 2007.

[71] N. Neophytou and H. Kosina, "Atomistic simulations of low-field mobility in Si nanowires: Influence of confinement and orientation," Phys. Rev. B, 84, 085313, 2011.

[72] G. T. Loh, E. H. T. Teo, B. K. Tay, "Phonon localization around vacancies in graphene nanoribbons," Diamond & Related Materials, vol. 23, pp. 88-92, 2012.

[73] J. F. Rodriguez-Nieva, R. Saito, S. D. Costa, and M. S. Dresselhaus, "Effect of ^{13}C isotope doping on the optical phonon modes in graphene: Localization and Raman spectroscopy," Phys. Rev. B, vol. 85, 245406, 2012.

[74] H. W. Kim, W. Ko, J. Y. Ku, I. Jeon, D. Kim, H. Kwon, Y. Oh, S. Ryu, Y. Kuk, S. W. Hwang, H. Suh, "Nanoscale control of phonon excitations in graphene," Nat. Commun., 6, 7528, 1–5, 2015.

[75] J.-W. Jiang, N. Yang, B.-S. Wang, and T. Rabczuk, "Modulation of thermal conductivity in kinked silicon nanowires: Phonon interchanging and pinching effects," Nano Lett., vol. 13, pp. 1670-1674, 2013.

[76] J. H. Seol, I. Jo, A. L. Moore, L. Lindsay, Z. H. Aitken, M. T. Pettes, X. Li, Z. Yao, R. Huang, D. Broido, N. Mingo, R. S. Ruoff, and L. Shi, "Two-dimensional phonon transport in supported graphene," Science 328, 213, 2010.